JCSE The Journal of Corrosion Science and Engineering
ISSN 1466-8858 Volume 16, Preprint 38 Submitted 7 May 2013

Systemic Assessment of Corrosion Rates of Aluminum-Manganese Alloys in Sea Water Based on Alloy Compositions and Initial Weights

C. I. Nwoye[1], N. E. Idenyi[2], F. Asuke[3], and V. S. Aigbodion[4]

[1]Department of Metallurgical and Materials Engineering, Nnamdi Azikiwe University, Awka, Nigeria.
[2]Department of Industrial Physics, Ebonyi State University, Abakaliki, Nigeria.
[3]Department of Metallurgical and Materials Engineering, Ahmadu Bello University, Zaria Nigeria.
[4]Department of Metallurgical and Materials Engineering, University of Nigeria, Nsukka, Enugu State Nigeria.
*Corresponding author: aigbodionv@yahoo.com (V.S Aigbodion)

Abstract

The corrosion rates of Aluminum-Manganese alloys in sea water have been ascertained based on alloy compositions and initial weights, using a derived model. The validity of the two- factorial derived model;$\beta = 0.0085\alpha 3 - 0.067\alpha 2 + 0.1582\ \alpha + 74000\ \gamma 2 - 1835\ \gamma + 11.278$ is rooted on the core expression: $1.3514 \times 10\text{-}5\ \beta + 9.0541 \times 10\text{-}7\ \alpha 2 + 0.0248\ \gamma = 1.1419 \times 10\text{-}7\ \alpha 3 + 2.1378 \times 10\text{-}6\ \alpha + \gamma 2 + 1.5206 \times 10\text{-}4$ where both sides of the expression are correspondingly approximately equal.

Keywords: Alloy, Weight loss, Acid corrosion

1. INTRODUCTION

Corrosion of pipelines and allied engineering structures has remained one of the main problems in oil and gas industries. This has always resulted in huge economic set back due to large sum of money spent trying to combat it. This necessitates the need to develop engineering materials that are corrosion resistant to avoid abrupt failure of the engineering structures. Studies [1] have shown that malfunctioning of engineering structures and equipment due to corrosion result from tragic carelessness in plumbing, equipment manufacture and installation, with possibility of explosion, fire and spread of toxic materials in living environment. This is accompanied by some costs such as shut down of plants due to replacement of corroded equipment, impurity in processed products due to corrosion, waste of the products of those vessels which are attacked by corrosion, replacement of corroded equipment as well as disturbance in processes due to equipment corrosion. The research indicates that about 70 percent of losses can be prevented by observing related principles and instructions.

Researchers [2-4] have shown that the corrosion behaviour of metals which is governed by the same basic kinetic and thermodynamic principles is not always predictable under the constantly changing environmental conditions in which they are put in service. It has been reported [5] that the stability of metals or alloys in an aggressive environment basically depends on the protective properties of organic or inorganic films as well as on the layer of corrosion products. The scientists concluded that the ability of films to act as controlling barriers against different kinds of corrosion attack is dependent on film properties such as chemical composition, adhesion, conductivity, solubility, morphology and hygroscopicity. Related studies [6, 7] reported that the highlighted characteristic of films in turn depends on environmental variables such as atmospheric conditions, type and amount of pollutants as well as wet-dry cycle, the chemical composition and metallurgical history of the metals or alloys and physicochemical properties of coating.

Report [6] has shown the need to know the specific corrosion rates of different metals and alloys in different application environment in order to know the materials that can withstand outdoor structural applications.

Aluminium alloys are normally used as sacrificial anodes in protecting steel structures in sea water because of their good current conductivity, since they can supply a large number of electrons for protection per unit mass. The demerit of applying pure aluminium as sacrificial anode is its ease of

ISSN 1466-8858 Volume 16, Preprint 35 submitted 17 May 2013

passivation through formation of oxide films on its surface. This invariably prevents contact between the metal and environment [7, 8].

Comparative analysis [8] of the service performance evaluation of aluminium, magnesium and zinc in terms of their applications as sacrificial anode in sea water environment gives aluminium preference over the other two basically because Al alloys have large electrochemical equivalents and low density. The researcher also reported that they are not wastefully consumed and possesses better current output.

Aluminium has been shown [9] to have almost the same electrode potential as $MnAl_6$ formed from Al and Mn and this compound is capable of dissolving iron which reduces the detrimental effect of Mn. Commercial Al-Mn alloys contains up to 1.25% manganese although the maximum solid solubility of this element in aluminium is as high as 1.82%. This limitation was imposed because the presence of iron as impurity reduces the solubility and there is a danger that large primary particles of $MnAl_6$ will form with a disastrous effect on local ductility.

Al-Mn alloys belong to the 3xxx series of alloys which are used for the manufacture of *roofing sheets, cans for beverage industries and cooking utensils* [9]. These sheets are subject to corrosion because of the presence of moisture and oxygen in the atmosphere. The corrosion of this alloy is due to the strong affinity aluminium has for oxygen which results to its oxidation and subsequent formation of oxide film. Ekuma et al. [10] reported that with time, this film becomes passive to further oxidation and stable in aqueous media when the pH is between 4.0 and 8.5. It is important to state that the passive films can break and fall of, hence exposing the surface of the alloy to further corrosion. The aim of this work is to assess the corrosion rates of aluminium-manganese alloys exposed to sea water based on alloy compositions and initial weights. The compositions of the alloys vary due to different Mn input on aluminum matrix.

2. MATERIALS AND METHODS

Materials used for the experiment [11] are virgin aluminium of 99% purity and pure granulated manganese. The other materials used were acetone, sodium chloride, distilled water, beakers and measuring cylinders. The equipment used was lathe machine, drilling machine, crucible furnace and analytical digital weighing machine.

2.1 Specimen preparation and experimentation

Computation for each of the Al-Mn alloy compositions was carefully worked out, and the alloying materials charged into the surface crucible furnace. The molten alloy was cast into rods and allowed to cool in air (at room temperature). The cooled rods were machined to specific dimensions, cut into test samples and weighed. Each sample coupon was drilled with 5mm drill bit to provide hole for the suspension of the strings. The surface of each of the test coupons was thoroughly polished with emery cloth [11].

The method adopted for this phase of the research [11] is the weight loss technique. The test coupons were exposed to the atmosphere and withdrawn after a known period of time. The withdrawn coupons were washed with distilled water, cleaned with acetone and dried in open air before weighing to determine the final weight.

2.2 Model formulation

Experimental data obtained from research work [11] were used for this work. Computational analysis of these data shown in Table 1, gave rise to Table 2-5 which indicate that;

$$K\beta + S_e\alpha^2 + N_e\gamma = N\alpha^3 + S\alpha + \gamma^2 + \theta \quad (1)$$

Introducing the values of K, N, S_e, S, N_e, and θ into equation (1)

$$1.3514 \times 10^{-5}\beta + 9.0541 \times 10^{-7}\alpha^2 + 0.0248\gamma = 1.1419 \times 10^{-7}\alpha^3 + 2.1378 \times 10^{-6}\alpha + \gamma^2 + 1.5206 \times 10^{-4} \quad (2)$$

JCSE The Journal of Corrosion Science and Engineering
ISSN 1466-8858 Volume 16, Preprint 35 submitted 17 May 2013

$$\beta = \left(\frac{1.1419 \times 10^{-7}\,\alpha^3 - 9.0541 \times 10^{-7}\,\alpha^2 + 2.1378 \times 10^{-6}\,\alpha + \gamma^2 - 0.0248\,\gamma + 1.5206 \times 10^{-4}}{1.3514 \times 10^{-5}} \right) \quad (3)$$

$$\beta = 0.0085\alpha^3 - 0.067\alpha^2 + 0.1582\,\alpha + 74000\,\gamma^2 - 1835\,\gamma + 11.278 \quad (4)$$

Where

K = 1.3514×10^{-5}; Corrosion coefficient of the Al-Mn alloy exposed in sea water for 336 hrs (determined using C-NIKBRAN [12])

N = 1.1419×10^{-7}; Third order alloy degradability coefficient due to exposure in sea water for 336 hrs (determined using C-NIKBRAN [12])

S_e= 9.0541×10^{-7}; Second order alloy degradability coefficient due to exposure in sea water for 336 hrs (determined using C-NIKBRAN [12])

S = 2.1378×10^{-6}; First order alloy degradability coefficient due to exposure in sea water for 336 hrs (determined using C-NIKBRAN [12])

N_e = 0.0248; Film solubility- adhesion ratio during alloy exposure in sea water for 336 hrs hrs (determined using C-NIKBRAN [12])

(θ) = 1.5206×10^{-4}: Al-Mn alloy oxidation coefficient (determined using C-NIKBRAN [12])

(β)= Corrosion rate (mm/yr)

(α) = Conc. of Mn added (to aluminum matrix) (%)

(γ) = Initial weight of alloy (kg)

3. BOUNDARY AND INITIAL CONDITIONS

Consider solid Al-Mn alloy exposed to sea water environment and interacting with some corrosion-induced agents. The sea water is assumed to be affected by unwanted dissolved gases. Range of Mn addition: 1 – 4%. Initial weight range considered: 0.0121-0.0129 kg (12.0754-12.9233g). Purity of aluminium used: 99%. Details of experiment and other process conditions are as stated in the experimental technique [11].

The boundary conditions are: aerobic environment to enhance Al-Mn alloy oxidation (since the sea water contains oxygen. At the bottom of the exposed alloy, a zero gradient for the gas scalar are assumed. The exposed alloy is stationary. The sides of the solid are taken to be symmetries.

4. RESULTS AND DISCUSSION

The sea water environment is known to contain the aggressive chloride ion and hence represent a positively saline environment. Results generated from the previous work [11] as shown in Table 1 indicate significant passivation in the aluminium alloys containing various quantities of Mn while they are exposed in sea water environment for 336 hrs. This is in accordance with past researches [13, 14, 15]. The highest corrosion rate was recorded on addition of 2% Mn to the aluminum matrix. Generally, the variation between the corrosion rate and Mn input is erratic while it varies directly as the alloy initial weight [11].

The derived model is equation (4). Computational analysis of Table 1 gave rise to Tables 2-5. The derived model is two-factorial, being essentially a constituent of two input process factors: alloy initial weight and Mn input (on aluminum matrix). This implies that the predicted corrosion rate for the Al-Mn alloy in sea water environment is dependent on just two factors: alloy initial weight and Mn input (on aluminum matrix).

The validity of the model is strongly rooted on equation (2) (core model equation) where both sides of the equation are correspondingly approximately equal. Table 5 also agrees with equation (2) following the values of $1.3514 \times 10^{-5}\,\beta + 9.0541 \times 10^{-7}\,\alpha^2 + 0.0248\,\gamma$ and $1.1419 \times 10^{-7}\,\alpha^3 + 2.1378 \times 10^{-6}\,\alpha + \gamma^2 + 1.5206 \times 10^{-4}$ evaluated from the experimental results in Table 1. Furthermore, the derived model was

validated by comparing the corrosion rate predicted by the model and that obtained from the experiment [11].

4.1.1 Computational Analysis

Computational analysis of the experimental and model-predicted corrosion rate was carried out to ascertain the degree of validity of the derived model. This was done by comparing the corrosion rate of Al-Mn alloy resulting from a unit % Mn input on aluminium matrix obtained by calculations involving experimental results, and predicted directly by the model.

The corrosion rate of Al-Mn alloy resulting from a unit % Mn input on aluminium matrix during the period of exposure in the sea water environment C_C (mm) was calculated from the equation;

$$C_C = \Delta\beta / \Delta\alpha \quad (5)$$

$\Delta\beta$ = Change in the corrosion rates β_2, β_1
$\Delta\alpha$ = Change in the values of two Mn percent input α_2, α_1

Considering experimental results of points (1, 0.0048) and (2.5, 0.0216) for (α_1, β_1) and (α_2, β_2) respectively as in Fig. 3 and substituting them into equation (5), gives 0.0112 mm /yr $(\%)^{-1}$ as the corrosion rate resulting from a unit % Mn input on aluminium matrix. Also similar plot (as in Fig. 4) using model-predicted results of points (1, 0.0049) and (2.5, 0.0237) for (α_1, β_1) and (α_2, β_2) respectively, and substituting them into equation (5) gives the corrosion rate resulting from a unit % Mn input on aluminium matrix as 0.0125 mm /yr $(\%)^{-1}$. This is the model-predicted corrosion rate resulting from a unit % Mn input on aluminium matrix.

4.1.2. Statistical analysis

Statistical analysis of model-predicted and experimentally evaluated corrosion rate for each value of alloy initial weight and composition considered shows a standard error (STEYX) of 0.0130 & 0.0126 % and 0.0155 & 0.0158 % respectively. The standard error was evaluated using a Microsoft Excel [16].

The correlations between corrosion rate and alloy initial weight as well as corrosion rate and concentration of Mn added to Al matrix as obtained from experiment [11] and derived model were calculated by considering the coefficients of determination R^2 from Figs. 1-4, using the equation;

$$R = \sqrt{R^2} \quad (6)$$

The evaluated correlations are shown in Tables 6 and 7. The model was also validated by comparing its results of evaluated correlations between corrosion rate and alloy initial weight as well as corrosion rate and concentration of Mn added to Al matrix with that evaluated using experimental. Tables 4 and 5 show that the correlation results from experiment and derived model are in proximate agreement.

4.1.3 Graphical Analysis

Results predicted by the model was plotted; corrosion rate against alloy initial weight and conc. of Mn input on Al matrix respectively along with results from the experiment to analyze its spread and trend relative to results from experiment.

Comparative graphical analysis of Figs. 5 and 6 shows very close alignment of the curves from derived model and experiment. It is strongly believed that the degree of alignment of these curves is indicative of the proximate agreement between ExD and MoD predicted results.

4.1.4 Deviational Analysis

Critical comparative analysis of corrosion rate from the experiment [11] and derived model revealed deviations on the part of the model-predicted values relative to values obtained from the experiment. This is attributed to the fact that the surface properties of the alloy and the physiochemical interaction between the alloy and corrosion induced agents (in the sea water) were not considered during the model formulation. This necessitated the introduction of correction factor, to bring the model-predicted corrosion

rate to those of the corresponding experimental values. Deviation (Dn) of model-predicted corrosion rate from that of the experiment [11] is given by

$$Dn = \left(\frac{Pe - Ee}{Ee}\right) \times 100 \quad (7)$$

Correction factor (Cr) is the negative of the deviation i.e

$$Cr = -Dn \quad (8)$$

Therefore

$$Cr = -\left(\frac{Pe - Ee}{Ee}\right) \times 100 \quad (9)$$

Where

Pe = Model-predicted corrosion rate (mm/yr)
Ee = Corrosion rate obtained from experiment [11] (mm/yr)
Cr = Correction factor (%)
Dn = Deviation (%)

Introduction of the corresponding values of Cr from equation (9) into the model gives exactly the corresponding experimental corrosion rate.

Figs. 7 and 8 show that the maximum deviation of the mode-predicted corrosion rate from the corresponding experimental values is less than 31%. These figures show that least and highest magnitudes of deviation of the model-predicted corrosion rate (from the corresponding experimental values) are -1.06 and + 30.77 % which corresponds to corrosion rates: 0.0372 and 0.0136 mm/yr, conc. of Mn input (on Al matrix): 2 and 4% and alloy initial weight; 0.0129 and 0.0121 kg respectively.
Comparative analysis of Figs. 7-10 indicates that the orientation of the curve in Figs. 9 and 10 is opposite that of the deviation of model-predicted corrosion rate (Figs. 7 and 8). This is because correction factor is the negative of the deviation as shown in equations (8) and (9). It is believed that the correction factor takes care of the effects of the surface properties of the alloy and physiochemical interaction between the alloy and corrosion induced agents (in the sea water) which were not considered during the model formulation. Figs. 9 and 10 indicate that the least and highest magnitudes of correction factor to the model-predicted corrosion rate are + 1.06 and -30.77 % which corresponds to corrosion rates: 0.0372 and 0.0136 mm/yr, conc. of Mn input (on Al matrix): 2 and 4% and alloy initial weight; 0.0129 and 0.0121 kg respectively.

It is important to state that the deviation of model predicted results from that of the experiment is just the magnitude of the value. The associated sign preceding the value signifies that the deviation is deficit (negative sign) or surplus (positive sign).

5. CONCLUSIONS

The corrosion rates of aluminum-manganese alloys in sea water have been predicted based on alloy compositions and initial weights using a derived model. The validity of the derived model; is rooted on the core expression: $1.3514 \times 10^{-5} \beta + 9.0541 \times 10^{-7} \alpha^2 + 0.0248 \gamma = 1.1419 \times 10^{-7} \alpha^3 + 2.1378 \times 10^{-6} \alpha + \gamma^2 + 1.5206 \times 10^{-4}$ where both sides of the expression are correspondingly approximately equal. Statistical analysis of model-predicted and experimentally evaluated corrosion rate for each value of % Mn input (to aluminium matrix) and alloy initial weight considered shows a standard error of 0.0155 & 0.0158 % and 0.0130 & 0.0126 % respectively. The corrosion rate resulting from a unit % Mn input on aluminium matrix (within a range 1-2.5%) as predicted by derived model and obtained from experiment are 0.0125 and 0.0112 mm/yr $(\%)^{-1}$. Deviational analysis indicates that the model will operate a best-fit application within a Mn input values 1 and 2% corresponding to deviations 2.08 and 1.06 % respectively.

JCSE The Journal of Corrosion Science and Engineering
ISSN 1466-8858 Volume 16, Preprint 35 submitted 17 May 2013

REFERENCES

[1]Samimi, A., and Zarinabadi, S. (2011). An Analysis of Polyethylene Coating Corrosion in Oil and Gas Pipelines. Journal of American Science 7(1):1032- 1036.
[2]Atkins, P. W. (1994). Physical Chemistry, 5th Edition Oxford University Press.
[3]Mark L. (1999).Introduction to Physical Chemistry, 3rd Edition, Low Price Editions, Cambridge University Press, USA.
[4]Logan, H. L. (1970).Basic Corrosion: Stress Corrosion, NACE Press, USA.
[5]Stratmann, M., Bohnenkamp, K., and Engell, W. J. (1983). An Electrochemical Study of Phase Transitions in Rust Layers Corros. Sci.., 23:969-985.
[6]Ekuma, C. E., and Idenyi, N. E. (2007). Statistical Analysis of the influence of Environment on Prediction of Corrosion from its Parameters. Res. J. Phy., USA, 1(1):27-34.
[7]Stratmann, S. G., and Strekcel, H. (1990). On the Atmospheric Corrosion of Metals which are Covered with Thin Electrolyte Layers. II. Experimental Results. Corros. Sci.., 30:697-714.
[8] Yaro, S. A., Muazu, A., and Kasim, A. (2010). Effect of Magnesium Addition on the Performance of Aluminium as Sacrificial Anode for Mild Steel Protection in Sea Water, JMME. 5(2):22-29.
[9[Polmear, I., J. (1981). Light Alloys. Edward Arnold Publishers Ltd.
[10]Ekuma, C. E., Idenyi, N. E., and Umahi, A. E. (2007). The Effects of Zinc Addition on the Corrosion Susceptibility of Aluminium Alloys in Various Tetraoxosulphate (vi) Acid Environments. J. of Appl. Sci., 7(2):237-241.
[11]Idenyi, N. E., Ogah, S. P. I., and Mbazor, J. C. (2010). Corrosion Behaviour of Al-Mn Binary Alloy Systems in Selected Environments. JMME. 5(1):37-42.
[12]Nwoye, C. I. (2008). C-NIKBRAN-Data Analytical Memory (Software).
[13]Ekuma, C. E., Idenyi, N. E., and Onwu, F. K., Umahi, A. E. (2008). The Influence of Media Concentrations On the Passivation Layer Characteristics of Al-Zn Alloy in Brine Environment. Asian J. Res., Pakistan 1(2):113-121.
[14]Idenyi, N. E., Ekuma, C. E., and Owate, I. O. (2006). The Influence of Alloy Composition on the Passive Layer Characteristics Al-Zn Alloys Systems. Proceedings of Material Science and Technology 2006 Meeting and Exhibition, Cincinnati, Ohio, USA, Oct 15th -19th, pp. 613-617.
[15]Ijomah, M. N. C. (1991). Element and Corrosion and Protection Theory, Auto Century Publishing, Company Ltd. Enugu. pp. 113-132.
[16]Microsoft Excel, 2003 version.

ISSN 1466-8858 Volume 16, Preprint 35 submitted 17 May 2013

CAPTION OF TABLES

Table 1: Variation of corrosion rate of Al-Mn alloy with its initial weight and Mn input (on aluminum matrix)
Table 2: Evaluated variation of Al-Mn alloy initial weight with its corrosion rate and Mn input (on aluminum matrix).
Table 3: Evaluated values of $1.1419 \times 10^{-7}\ \alpha^3$, $9.0541 \times 10^{-7}\ \alpha^2$ and $2.1378 \times 10^{-6}\ \alpha$
Table 4: Evaluated values of γ^2 and $0.0248\ \gamma$ at constant 1.5206×10^{-4}

Table 5: Variation of $1.3514 \times 10^{-5}\ \beta + 9.0541 \times 10^{-7}\ \alpha^2 + 0.0248\ \gamma$ with $1.1419 \times 10^{-7}\ \alpha^3 + 2.1378 \times 10^{-6}\ \alpha + \gamma^2 + 1.5206 \times 10^{-4}$

Table 6: Comparison of the correlations between corrosion rate and alloy initial weight as evaluated from experimental and derived model results
Table 7: Comparison of the correlations between corrosion rate and concentration of Mn added to Al matrix

CAPTION OF FIGURES

Fig. 1: Coefficient of determination between corrosion rate and alloy initial weight as obtained from the experiment
Fig. 2: Coefficient of determination between corrosion rate and alloy initial weight as predicted by derived model.

Fig. 3: Coefficient of determination between corrosion rate and concentration of Mn added to Al matrix as obtained from the experiment
Fig. 4: Coefficient of determination between corrosion rate and concentration of Mn added to Al matrix as predicted by derived model

Fig. 5: Comparison of the corrosion rate (relative to its alloy initial weight) as obtained from experiment and derived model.
Fig. 6: Comparison of the corrosion rate (relative to the conc. of Mn input on Al matrix) as obtained from experiment and derived model.
Fig. 7: Variation of model-predicted corrosion rate (relative to alloy initial weight) with its associated deviation from experimental values

Fig. 8: Variation of model-predicted corrosion rate (relative to the conc. of Mn input on Al matrix) with its associated deviation from experimental values
Fig. 9: Variation of model-predicted corrosion rate (relative to alloy initial weight) with its associated correction factor
Fig. 10: Variation of model-predicted corrosion rate (relative to the conc. of Mn input on Al matrix) with its associated correction factor

ISSN 1466-8858 Volume 16, Preprint 35 submitted 17 May 2013

LIST OF TABLES

Table 1: Variation of corrosion rate of Al-Mn alloy with its initial weight and Mn input (on aluminum matrix)

(β) (mm/yr)	(α) (%)	(γ) (g)
0.0048	1.0	12.6150
0.0376	2.0	12.9233
0.0216	2.5	12.8134
0.0056	3.0	12.6152
0.0104	4.0	12.0754

Table 2: Evaluated variation of Al-Mn alloy initial weight with its corrosion rate and Mn input (on aluminum matrix).

(β) (mm/yr)	(α) (%)	(γ) (kg)
0.0048	1.0	0.0126
0.0376	2.0	0.0129
0.0216	2.5	0.0128
0.0056	3.0	0.0126
0.0104	4.0	0.0121

Table 3: Evaluated values of $1.1419 \times 10^{-7}\ \alpha^3$, $9.0541 \times 10^{-7}\ \alpha^2$ and $2.1378 \times 10^{-6}\ \alpha$

$1.1419 \times 10^{-7}\ \alpha^3$	$9.0541 \times 10^{-7}\ \alpha^2$	$2.1378 \times 10^{-6}\ \alpha$
1.1419×10^{-7}	9.0541×10^{-7}	21.378×10^{-7}
9.1352×10^{-7}	36.2164×10^{-7}	42.756×10^{-7}
17.8422×10^{-7}	56.5881×10^{-7}	53.445×10^{-7}
30.8313×10^{-7}	81.4869×10^{-7}	64.134×10^{-7}
73.0816×10^{-7}	144.8656×10^{-7}	85.512×10^{-7}

Table 4: Evaluated values of γ^2 and $0.0248\ \gamma$ at constant 1.5206×10^{-4}

(γ^2)	$0.0248\ \gamma$	1.5206×10^{-4}
1587.6×10^{-7}	3124.8×10^{-7}	1520.6×10^{-7}
1664.1×10^{-7}	3199.2×10^{-7}	1520.6×10^{-7}
1638.4×10^{-7}	3174.4×10^{-7}	1520.6×10^{-7}
1587.6×10^{-7}	3124.8×10^{-7}	1520.6×10^{-7}
1464.1×10^{-7}	3000.8×10^{-7}	1520.6×10^{-7}

Table 5: Variation of $1.3514 \times 10^{-5}\ \beta + 9.0541 \times 10^{-7}\ \alpha^2 + 0.0248\ \gamma$ with $1.1419 \times 10^{-7}\ \alpha^3 + 2.1378 \times 10^{-6}\ \alpha + \gamma^2 + 1.5206 \times 10^{-4}$

$1.3514 \times 10^{-5}\ \beta + 9.0541 \times 10^{-7}\ \alpha^2 + 0.0248\ \gamma$	$1.1419 \times 10^{-7}\ \alpha^3 + 2.1378 \times 10^{-6}\ \alpha + \gamma^2 + 1.5206 \times 10^{-4}$
0.3135×10^{-3}	0.3131×10^{-3}
0.3240×10^{-3}	0.3237×10^{-3}
0.3234×10^{-3}	0.3230×10^{-3}
0.3207×10^{-3}	0.3203×10^{-3}
0.3147×10^{-3}	0.3143×10^{-3}

ISSN 1466-8858 Volume 16, Preprint 35 submitted 17 May 2013

Table 6: Comparison of the correlations between corrosion rate and alloy initial weight as evaluated from experimental and derived model results

Analysis	Based on alloy initial weight	
	ExD	D-MoD
CORREL	0.9975	0.9993

Table 7: Comparison of the correlations between corrosion rate and concentration of Mn added to Al matrix

Analysis	Based on conc. of Mn input on Al matrix	
	ExD	D-MoD
CORREL	0.9988	0.9999

ISSN 1466-8858 Volume 16, Preprint 35 submitted 17 May 2013

LIST OF FIGURES

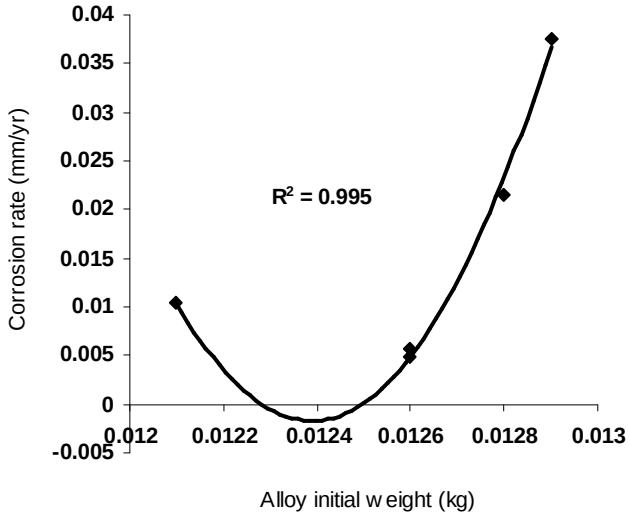

Fig. 1: Coefficient of determination between corrosion rate and alloy initial weight as obtained from the experiment

ISSN 1466-8858
submitted 17 May 2013

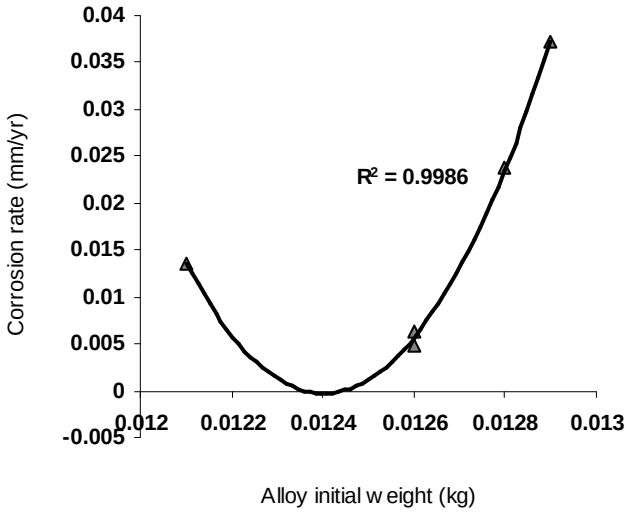

Fig. 2: Coefficient of determination between corrosion rate and alloy initial weight as predicted by derived model.

ISSN 1466-8858
submitted 17 May 2013

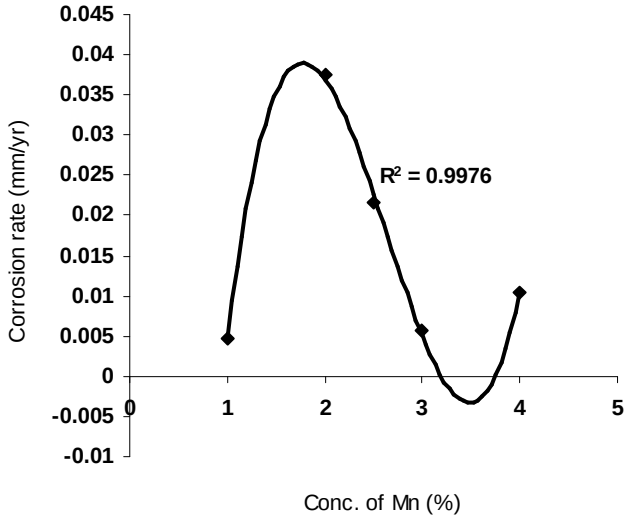

Fig. 3: Coefficient of determination between corrosion rate and concentration of Mn added to Al matrix as obtained from the experiment

ISSN 1466-8858
submitted 17 May 2013

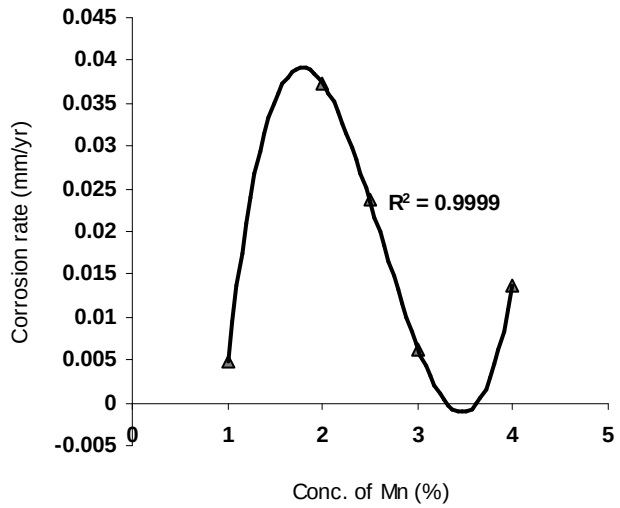

Fig. 4: Coefficient of determination between corrosion rate and concentration of Mn added to Al matrix as predicted by derived model

ISSN 1466-8858
submitted 17 May 2013

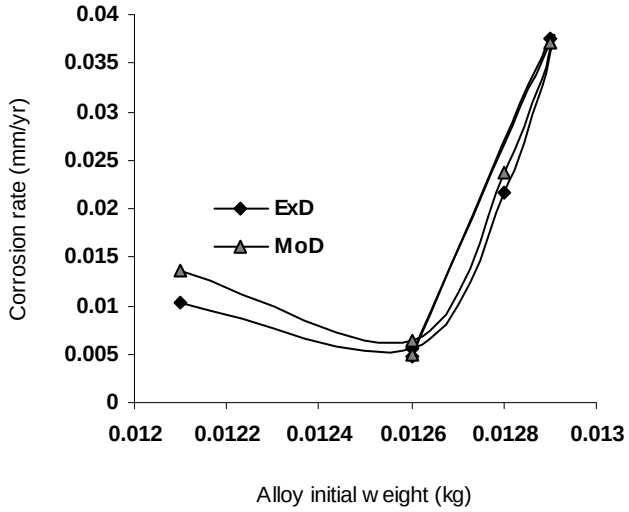

Fig. 5: Comparison of the corrosion rate (relative to its alloy initial weight) as obtained from experiment and derived model.

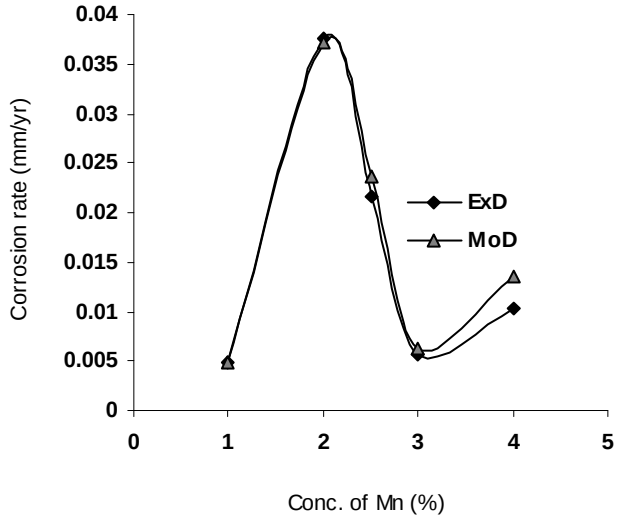

Fig. 6: Comparison of the corrosion rate (relative to the conc. of Mn input on Al matrix) as obtained from experiment and derived model.

ISSN 1466-8858 Volume 16, Preprint 35 submitted 17 May 2013

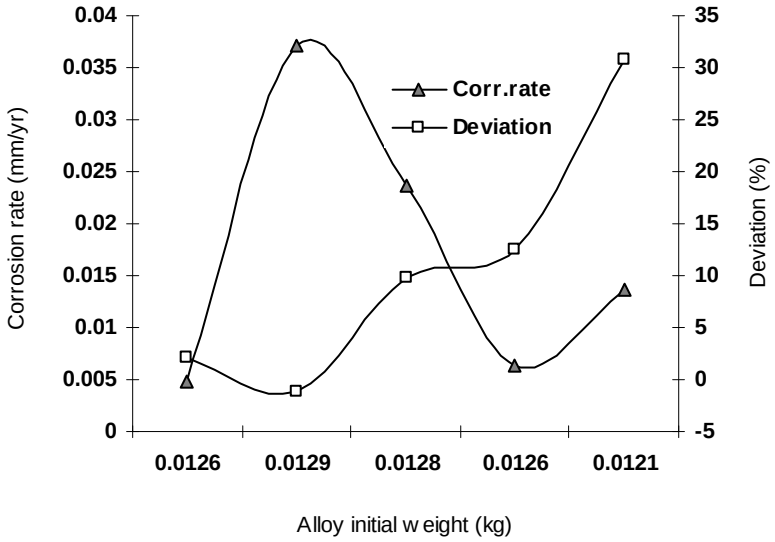

Fig. 7: Variation of model-predicted corrosion rate (relative to alloy initial weight) with its associated deviation from experimental values

ISSN 1466-8858
ubmitted 17 May 2013

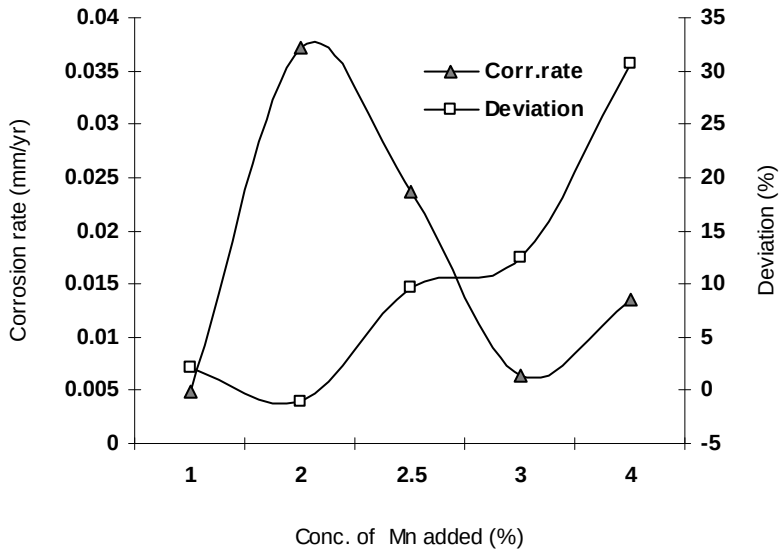

Fig. 8: Variation of model-predicted corrosion rate (relative to the conc. of Mn input on Al matrix) with its associated deviation from experimental values

ISSN 1466-8858
submitted 17 May 2013

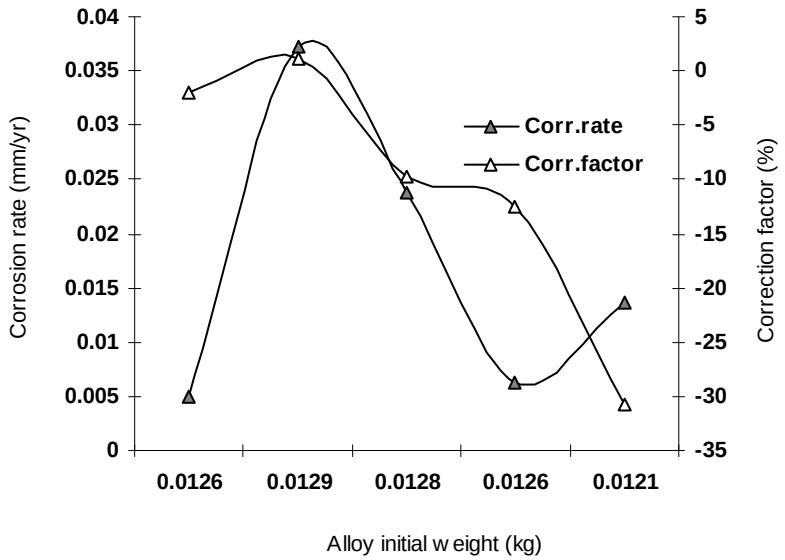

Fig. 9: Variation of model-predicted corrosion rate (relative to alloy initial weight) with its associated correction factor

ISSN 1466-8858 submitted 17 May 2013

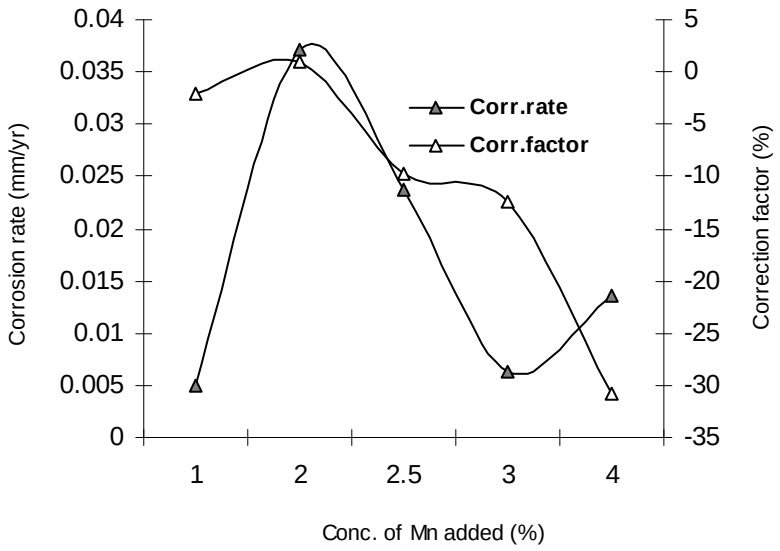

Fig. 10: Variation of model-predicted corrosion rate (relative to the conc. of Mn input on Al matrix) with its associated correction factor